© 2020. Published by The Company of Biologists Ltd | Journal of Experimental Biology (2020) 223, jeb214916. doi:10.1242/jeb.214916

METHODS & TECHNIQUES

A fast and effective method for dissecting parasitic spores: myxozoans as an example

Qingxiang Gu[1], Yang Liu[1,2], Yanhua Zhai[1,2] and Zemao Gu[1,2,*]

ABSTRACT

Disassembling parasitic spores and acquiring the main subunits for analysis is a prerequisite for a deep understanding of the basic biology of parasites. Herein, we present a fast and efficient method to dissect myxospores in a few steps, which mainly involves sonication, and sucrose and Percoll density gradient ultracentrifugation. We tested our method on three myxozoan species and demonstrate that this method allows the dismembering of myxospores, and the isolation of intact and clean nematocysts and shell valves within 2 h at low cost. This new tool will facilitate subsequent analyses and enable a better understanding of the ecological and evolutionary significance of parasitic spores.

KEY WORDS: Dissection, Antigens, Parasites, Nematocysts

INTRODUCTION

Many parasites are known to be spore forming and use the sporic stage for reproduction, development and stress resistance (Coppens, 2019; Goodgame, 1996). These spores usually exert their function by the cooperation of several subunits or by using quasi-independent ones independently. Thus, dismembering these spores and acquiring the main subunits is an important prerequisite for investigations addressing various questions concerning their evolution and cell biology.

In light of this objective, renewed attention was given to investigation of the composition and fine structure of spore subunits (Ben-David et al., 2016; Vávra et al., 2016), which might help to detect new antigens for immuno-protection studies (Xu et al., 2006; Yang et al., 2017), to understand the mechanism of assembly/invasion (Jaroenlak et al., 2018; Yang et al., 2018), and to develop control strategies or screen drugs (Aldama-Cano et al., 2018). From a methodological perspective, because most of the spores are extremely small (micrometer sized), spore dissection remains a challenge and only limited studies have explored this approach in parasitology. For instance, the manual dissection of fungal spores can be conducted on a tetrad dissection microscope. This method, although effective, requires well-trained personnel and is limited to ascospore-producing species (Amberg et al., 2005). Additionally, a tailored dielectrophoresis-based microfluidic has been developed to specifically isolate the nematocysts of myxozoan *Ceratonova shasta* infecting salmon and trout (Piriatinskiy et al., 2017). However, the microfluidic technique has the drawback of high cost, complex operational control/chip design and as yet little standardization in this field (Halldorsson et al., 2015; Velve-Casquillas et al., 2010). Another issue is the possible electrolysis caused by the electric fields themselves (Mark et al., 2010). Thus, a method for dissecting spores and isolating the main subunits is needed.

Myxozoans are widespread endoparasitic cnidarians (Atkinson et al., 2018; Dyková et al., 2011; Naldoni et al., 2019), which are miniaturized and morphologically simplified. Myxospores infecting the invertebrate hosts only consist of polar capsules (referred to as nematocysts below), shell valves and sporoplasms (Morsy et al., 2016). Although those unique cell types are present in myxozoans, their basic cell biology has been understudied, contributing to the enigmatic status of myxozoans. In the past decades, extensive efforts have been made to isolate nematocysts from free-living cnidarians (anthozoans, cubozoans, scyphozoans and hydrozoans). These studies have served as an important basis for the interpretation of nematocyst biology, including their structure, function, venom toxicology/pharmacology/bioactivity and omics (Balasubramanian et al., 2012; Brinkman et al., 2015; Marino et al., 2009; Ponce et al., 2016; Schlesinger et al., 2008). However, compared with those of their free-living relatives, nematocysts of myxozoans have been less studied and there are currently no consensus methodologies for dissection and simultaneous acquisition of myxozoan main subunits. Our goal was to develop a new, fast and efficient method for myxospore dissection that can be utilized to isolate nematocysts and shell valves from representative species *Myxobolus honghuensis* Liu and Gu 2011 and *Myxobolus wulii* Landsberg and Lom 1991 infecting *Carassius auratus gibelio*; and *Thelohanellus kitauei* Egusa and Nakajima 1981 infecting *Cyprinus carpio*. This was achieved through spore purification by sucrose density gradient ultracentrifugation, spore disruption by sonication and nematocyst/shell valve isolation by Percoll density gradient ultracentrifugation. The nematocysts and shell valves obtained with the optimized protocol showed an intact structure and negligible contamination. The method presented here has the potential to improve our understanding of the basic biology of these enigmatic parasites, and may in addition help to shed light on segmentation research in a wider range of spore-forming parasites.

MATERIALS AND METHODS

Animals

Myxobolus honghuensis myxospores were obtained from infected allogynogenetic gibel carp *C. auratus gibelio* in Zoumaling Farm (Hubei, China). *Myxobolus wulii* myxospores were collected from *C. auratus gibelio* in Yellow Sand Port (Jiangsu Province, China). *Thelohanellus kitauei* myxospores were obtained from infected mirror carp *C. carpio* in Liuerbao Town (Shenyang, China). Infected fish were sent to the laboratory and held in aerated, large

[1]Department of Aquatic Animal Medicine, College of Fisheries, Huazhong Agricultural University, Wuhan, Hubei province 430070, People's Republic of China. [2]Hubei Engineering Technology Research Center for Aquatic Animal Diseases Control and Prevention, Wuhan, Hubei province 430070, People's Republic of China.

*Author for correspondence (guzemao@mail.hzau.edu.cn)

Q.G., 0000-0002-3694-3428; Z.G., 0000-0002-1278-4610

Received 17 September 2019; Accepted 27 March 2020

Journal of Experimental Biology (2020) 223, jeb214916. doi:10.1242/jeb.214916

square tanks overnight before a routinely performed parasitological examination. The maintenance and care of experimental animals complied with the National Institutes of Health guidelines for the humane use of laboratory animals. All experimental procedures involving fish were approved by the institution's animal care and use committee of the Huazhong Agricultural University, China.

Assembly of sucrose and Percoll density gradients

One sucrose and two Percoll density gradients (Percoll gradient 1 and 2) were assembled for downstream processes. For the sucrose density gradient, sucrose was dissolved in phosphate-buffered saline (PBS, 0.1 mol l^{-1}, adjusted to pH 7.2) to make 30%, 40%, 50% and 60% w/w sucrose solution (all sucrose density gradients are represented as weight concentration; see also below); 8 ml of each sucrose solution was placed into a chilled 50 ml tube using a 5 ml syringe equipped with 21-gauge stainless steel intramedic tubing (Bolige Industry and Trade Co., Ltd, Shanghai, China). Sucrose of lower concentration was placed first into the bottom of the tube, followed by the addition of higher concentration sucrose into the bottom to raise up the upper layer. For Percoll density gradient 1, Percoll was diluted in PBS to prepare 50%, 70% and 90% v/v Percoll solution (all Percoll density gradients are represented as volume concentration; see also below); 2 ml of each Percoll solution was added to the chilled 10 ml tube using the method described above. For Percoll density gradient 2, 100% Percoll stock solution was directly added to the 2 ml chilled tube. Each step in gradient preparation was handled carefully to avoid mixing the layers.

Isolation and purification of intact spores

Myxozoan cysts were excised from infected tissues (pharynx for *M. honghuensis*, liver for *M. wulii* and intestine for *T. kitauei*); 2–4 g of tissue were sliced into pieces and then homogenized by a hand-operated glass tissue grinder. Homogenate was suspended in PBS and then filtered through cotton gauze to remove aggregated tissues. The filtrate containing crude myxospores was washed in PBS 2 times at 1635 ***g*** for 15 min and resuspended in 8 ml PBS. The suspension was carefully added to the top of the 30%, 40%, 50% and 60% sucrose density gradient before centrifugation at 3200 ***g*** for 15 min. The liquid above the gradient was removed. The 40%/50% and 50%/60% interface that contained most of the spores was carefully collected with a Pasteur pipette. The collected liquid was washed with PBS 2 times at 1635 ***g*** for 15 min. The supernatant was removed with a pipette and the pellet that contained purified intact spores was resuspended in 10 ml PBS.

Spore dissection

The intact spore suspension was sub-packed in a 2 ml tube and sonicated with a microtip probe sonicator (JY92-IIN, Scientz Biotechnology, Ningbo, China) on ice for 3 min (on for 3 s and rest for 1 s) at 85 W output. Sonicated spore samples were concentrated by centrifugation at 2000 ***g*** for 5 min and resuspended in 4.5 ml PBS for downstream procedures.

Nematocyst isolation

A 1.5 ml sample of the sonicated spore suspension was carefully loaded onto the top of Percoll density gradient 1 (50%, 70% and 90% Percoll) by drawing the suspension into a Pasteur pipette and slowly releasing the solution above the 50% Percoll layer.

The gradient was subjected to centrifugation at 1470 ***g*** for 25 min and stopped with a slow break speed. After centrifugation, the white bands at the 50%/70% Percoll interface and the middle of the 70% Percoll layer were collected with a Pasteur pipette. The collected liquid was concentrated by centrifugation at 2000 ***g*** for 5 min and resuspended in 3 ml PBS, followed by secondary purification through Percoll density gradient 1. The final collected liquid containing the pure nematocysts was diluted with 1.5 ml PBS. The purity of the nematocyst suspension was assessed by light microscopy.

Shell valve isolation

A 0.5 ml sample of sonicated spore suspension was overlaid on Percoll density gradient 2 (100% Percoll) in a 2 ml chilled tube. The liquid was centrifuged at 6580 ***g*** for 15 min. After centrifugation, the white band located at the upper-middle layer of 100% Percoll was collected. The crude shell valves were collected by centrifugation at 2000 ***g*** for 5 min and immediately subjected to secondary purification through Percoll density gradient 2. The final collected liquid containing the pure valves was resuspended with 1.5 ml PBS. The purity of the shell valve suspension was assessed by light microscopy.

Evaluation of the effects of heat, salinity and various chemicals on spore and isolated nematocyst discharge

An Olympus BX53 light microscope, equipped with an Olympus DP73 digital camera (Olympus, Hamburg, Germany), was used to verify that spores and nematocysts of *M. honghuensis* were undischarged. Spores and nematocysts were then added to a 0.2 ml centrifuge tube and received the following treatments: 30 min heat treatment at 95°C; 3 min incubation with 0.4% urea (w/w); and 10 min incubation with 40‰ NaCl (w/w), 5% acetic acid (w/w), 20% ammonia (w/w), 70% ethanol (w/w), 10% sodium bicarbonate (w/w) or 10 mmol l^{-1} $CaCl_2$. The number of discharged and undischarged nematocysts was counted under the microscope at a magnification of ×40. At least 100 nematocysts were counted in each measurement and the discharge number was expressed as a percentage. All measurements were repeated 3 times on different preparations of spores and isolated nematocysts.

Evaluation of the effects of heavy metals on the discharge ability of spores and isolated nematocysts

Spores and nematocysts of *M. honghuensis* were then added to a 0.2 ml centrifuge tube and incubated for 30 min in 200 µl of a 10 mmol l^{-1} solution of $ZnSO_4$, $BaCl_2$, $FeCl_3$, $MnCl_2$ or $CdCl_2$. After incubation, the spores and nematocysts were checked for discharge. Then liquid containing heavy metals was removed and 0.4% urea was used to stimulate the discharge of spores and nematocysts; these were quantified as previously described. The significance of the differences between mean values was tested using one-way analysis of variance (ANOVA), followed by Bonferroni's or Dunnet's *post hoc* test.

Transmission electron microscopy

For transmission electron microscopy (TEM), nematocysts were fixed in 3% glutaraldehyde in 0.2 mol l^{-1} sodium cacodylate buffer (pH 7.2) at 4°C overnight and post-fixed in 2% OsO_4 buffered with the same solution for 4 h at the same temperature. After dehydration in an ascending ethanol series and propylene oxide, specimens were finally embedded in Epon812. Semi-thin sections were stained with Toluidine Blue. Ultrathin sections were double-stained with uranyl acetate and lead citrate, then examined and photographed by a 200 kV transmission electron microscope (Tecnai G20 TWIN, FEI Company, Hillsboro, OR, USA).

Journal of Experimental Biology (2020) 223, jeb214916. doi:10.1242/jeb.214916

RESULTS AND DISCUSSION

To determine the optimal method for myxospore dissection, we conducted a series of trial-and-error explorations and the final protocol involved four main steps: spore purification, spore disruption, nematocyst isolation and shell valve isolation (Fig. 1A). Briefly, myxozoan cysts were excised from infected tissues and myxospores were purified from the 40%/50% and 50%/60% interface of a 30%, 40%, 50%, 60% sucrose density gradient. Then, spores were disrupted by sonication for 3 min (on for 3 s and rest for 1 s) at 85 W electric power. Thereafter, by using 50%, 70%, 90% Percoll and 100% Percoll gradient, respectively, pure nematocysts (50%/70% interface and the middle of the 70% layer) and shell valves (upper of the 100% layer) were separated from the sonicated suspension.

More specifically, we first purified the spores from homogenized cysts (Fig. 2A,B) using the sucrose density gradient. For all three species tested in the present study, the optimal 30%, 40%, 50%, 60% sucrose density gradient centrifugation (Fig. 1A) showed similar stratification with three visible bands at the 30% layer, 40%/50% interface and 50%/60% interface (Fig. 1B). Upon examination by light microscopy, the 30% layer was found to contain trophozoites in the form of polysporic plasmodia. The 40%/50%

A

Main procedures	Isolation		
	Spores	Nematocyst	Valves
1. Homogenization of fish tissue	Homogenizer		
2. Filtration	Gauze, 2IS/28x28		
3. Washing with PBS	1635 ***g***, 15 min		
4. Isolation on sucrose gradient	3200 ***g*** 15 min	3200 ***g*** 15 min	3200 ***g*** 15 min
5. Sonication	NA	85 W, 3/1 3 min	85 W, 3/1 3 min
6. Isolation on Percoll gradient	NA	1470 ***g*** 25 min	6580 ***g*** 15 min
7. Secondary purification	NA	1470 ***g*** 25 min	6580 ***g*** 15 min
8. Washing with PBS	1635 ***g***, 15 min		

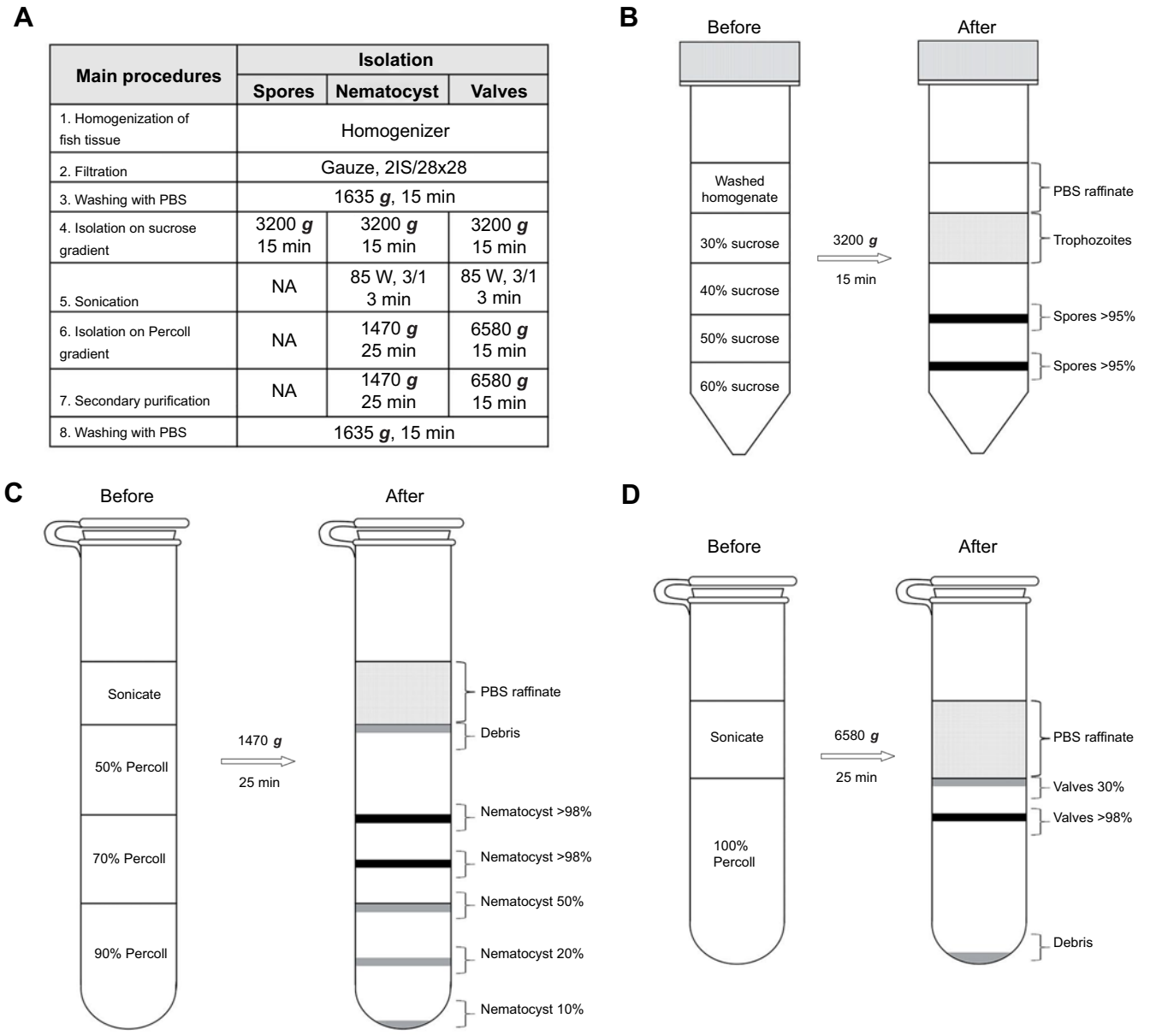

Fig. 1. Outline of the procedures for isolation of nematocysts and shell valves from myxozoans. (A) Steps in the isolation of whole spores, nematocysts and valves. (B) Isolation of spores using sucrose density gradient centrifugation, shown in more detail. The filtered homogenate was loaded on the top of the 30%, 40%, 50%, 60% (w/w) sucrose density gradient before centrifugation (3200 ***g***, 15 min). The spores (shown in black) were then collected from the 40%/50% and 50%/60% interface. (C) Isolation of nematocysts using Percoll density gradient centrifugation, shown in more detail. The sonicated spores were loaded on the top of the 50%, 70%, 90% (v/v) Percoll density gradient before centrifugation (1470 ***g***, 25 min). The nematocysts (shown in black) were then collected from the 50%/70% interface and the middle of the 70% layer. (D) Isolation of shell valves using Percoll density gradient centrifugation, shown in more detail. The sonicated spores were loaded on the top of 100% (v/v) Percoll before centrifugation (6580 ***g***, 25 min). The valves (shown in black) were then collected from the upper part of the 100% layer.

Journal of Experimental Biology (2020) 223, jeb214916. doi:10.1242/jeb.214916

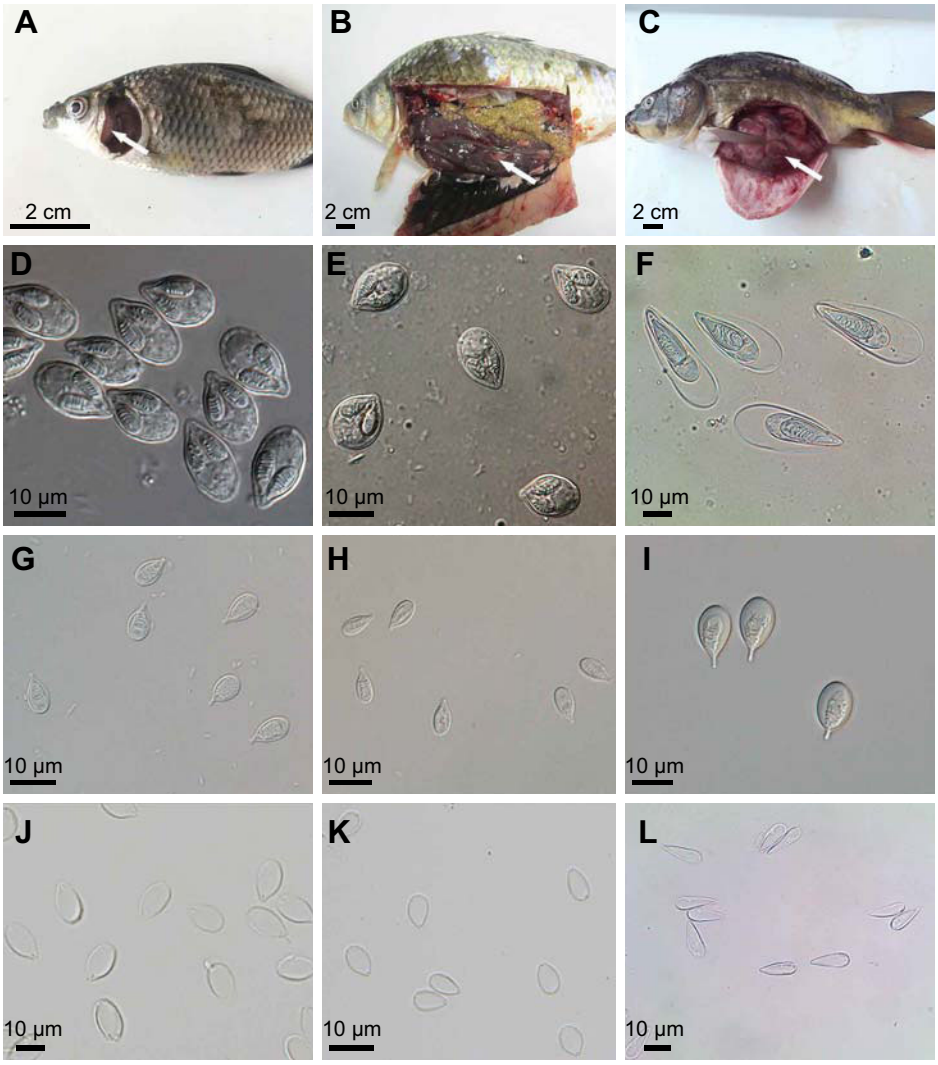

Fig. 2. Light micrographs of fish specimens, intact spores, isolated nematocysts and shells valves. (A–C) Allogynogenetic gibel carp *Carassius auratus gibelio* infected with *Myxobolus honghuensis* (A); *C. auratus gibelio* infected with *Myxobolus wulii* (B); mirror carp *Cyprinus carpio* infected with *Thelohanellus kitauei* (C). Cysts (white arrow) were observed. (D–F) Fresh spores of *M. honghuensis* (D), *M. wulii* (E) and *T. kitauei* (F). (G–I) Isolated nematocysts of *M. honghuensis* (G), *M. wulii* (H) and *T. kitauei* (I). (J–L) Isolated valves of *M. honghuensis* (J), *M. wulii* (K) and *T. kitauei* (L).

and 50%/60% interface contained intact spores with negligible contamination (Fig. 2D–F). For any suboptimal sucrose density gradient, the debris, mature spores and trophozoites will fail to be separated. These results suggest that by using the sucrose density gradient centrifugation described here, mature spores can be isolated from host debris and trophozoites with high purity and integrity, to provide materials for downstream spore disruption. To open the sutural ridge of the spores, we chose to sonicate the spore suspension with different parameter combinations of working time, pulse and output power. An optimal sonication protocol of power 85 W for 3 min (on for 3 s and rest for 1 s) (Fig. 1A) led to successful disruption of almost all of the spores, the sutural ridge of which was opened and the nematocysts dissociated. The free shell valves and nematocysts all remained intact. If the sonication was too ‘strong’ (e.g. long effective sonication times, high output power), the shell valves and nematocysts would be broken and the polar filaments would extrude. However, if the sonication was too ‘gentle’, the sutural ridge between the two valves was hardly opened because of low cavitation. Taken together, appropriate sonication can be used to rupture the myxospores and we prefer this method over SDS and proteolytic treatment (Piriatinskiy et al., 2017), because the physical treatment might minimally interfere with proteins and be more appropriate for some downstream analyses, e.g. proteomics or epitope analysis.

For nematocyst isolation, the final 50%, 70%, 90% Percoll gradient led to optimal results: nematocysts in an almost pure state (>98%) were collected from the 50%/70% interface and the middle of the 70% layer (Fig. 1C). After the secondary purification, which repeated the optimal Percoll gradient process, intact, clean and unextruded nematocysts (Fig. 2G–I) were successfully isolated from the three myxozoans. However, an inappropriate choice of centrifugation medium or gradient will result in a low purity of nematocysts or even fail to separate the nematocysts from the shell valves. For instance, by using a 40%, 45%, 50%, 55%, 60% sucrose density gradient, we could only collect nematocysts with a maximum purity of 70% (Fig. S1A), which is non-ideal. The density of nematocysts in the present case was estimated to be around 1.20254–1.22957 g ml^{-1} according to the stratification of nematocysts and density of sucrose solution with different mass fraction at 20°C (Honig, 2013). Based on the inferred nematocyst density, we further optimized the gradient to 45%, 47%, 49%, 52%, 60% sucrose and collected nematocysts with a maximum purity of 80% (Fig. S1B), which was an improvement but not optimal. Simply changing the medium to a Percoll gradient of 50%, 60%, 70%, 80%, 90%, 100% improved the maximum purity of isolated nematocysts to 90% (Fig. S1C), second only to the optimal 50%, 70%, 90% Percoll gradient. These results suggest that the present protocol is very effective for nematocyst isolation and confirm that

Journal of Experimental Biology (2020) 223, jeb214916. doi:10.1242/jeb.214916

Percoll is a better gradient medium with higher resolution and lower osmolarity compared with sucrose (Dunkley et al., 1986), while the latter can be used in density estimation.

To further study the nematocysts, we evaluated whether heat, high salinity and various chemicals can trigger the discharge of *M. honghuensis* spores/nematocysts, and whether heavy metals can affect the discharge response. Our results showed that heat, urea and ammonia successfully triggered the discharge of most spores and isolated nematocysts, whereas NaCl, acetic acid, ethanol, sodium bicarbonate and $CaCl_2$ did not (Table S1). The positive results with heat and the negative results with NaCl and sodium bicarbonate are in line with those reported by Glaser and Sparrow (1909), Hoffman et al. (1965) and Birsa et al. (2010). The positive result with urea is in accordance with the study of Molnár et al. (2009), but different from the findings of Birsa et al. (2010). The negative effect of ethanol on discharge is supported by the work of Glaser and Sparrow (1909) and Morabito et al. (2014) and in contrast to that of Birsa et al. (2010). Our results with acetic acid and ammonia are the same as those previously reported by Glaser and Sparrow (1909) and Birsa et al. (2010) and different from those of Morabito et al. (2014). This discrepancy may depend on the species specificity of the nematocysts, as found in previous studies (Birsa et al., 2010; Morabito et al., 2014). With regard to heavy metals, we showed that a 30 min exposure of spores/nematocysts to $ZnSO_4$, $BaCl_2$, $FeCl_3$, $MnCl_2$ or $CdCl_2$, dramatically impaired discharge of nematocysts (Table S2). This result is in line with those of Morabito et al. (2013a, 2014) and may be because heavy metals affect discharge by impairing ion flux via membrane transport systems, as already shown in *Pelagia noctiluca* (Morabito et al., 2013b). All in all, although the nematocyst discharge mechanism has not been fully determined, our findings support the osmotic theory, which states that an increase of the internal pressure of the capsule is required for discharge (Birsa et al., 2010). Additionally, the discharge ability of myxozoan nematocysts was used to evaluate the viability of spores (Molnár et al., 2009). Our results, for the first time, suggest that the discharge of myxozoan nematocysts is an independent process (Fig. S2) and inappropriate for evaluation of viability.

Furthermore, we performed TEM on the fine structure of isolated nematocysts. An inverted tubule was clearly observed (Fig. 3A,B,E,F,I) – at higher magnification, the tubule was shown to be hollow and filled with electron-dense particles (Fig. 3C,G). This is in accordance with previous reports that *Myxobolus* has an open tubule and we speculated the electron-dense particles might be the putative venom of *Myxobolus* (Ben-David et al., 2016; Piriatinskiy et al., 2017). An opercular cap was clearly visible at the top of nematocysts (Fig. 3D,H), indicating that the myxozoan nematocyst is atrichous isorhiza (Okamura et al., 2015). A higher magnification view of the nematocyst shell showed a trilaminar structure, with an outer electron-dense zone, an adjacent electron-lucent

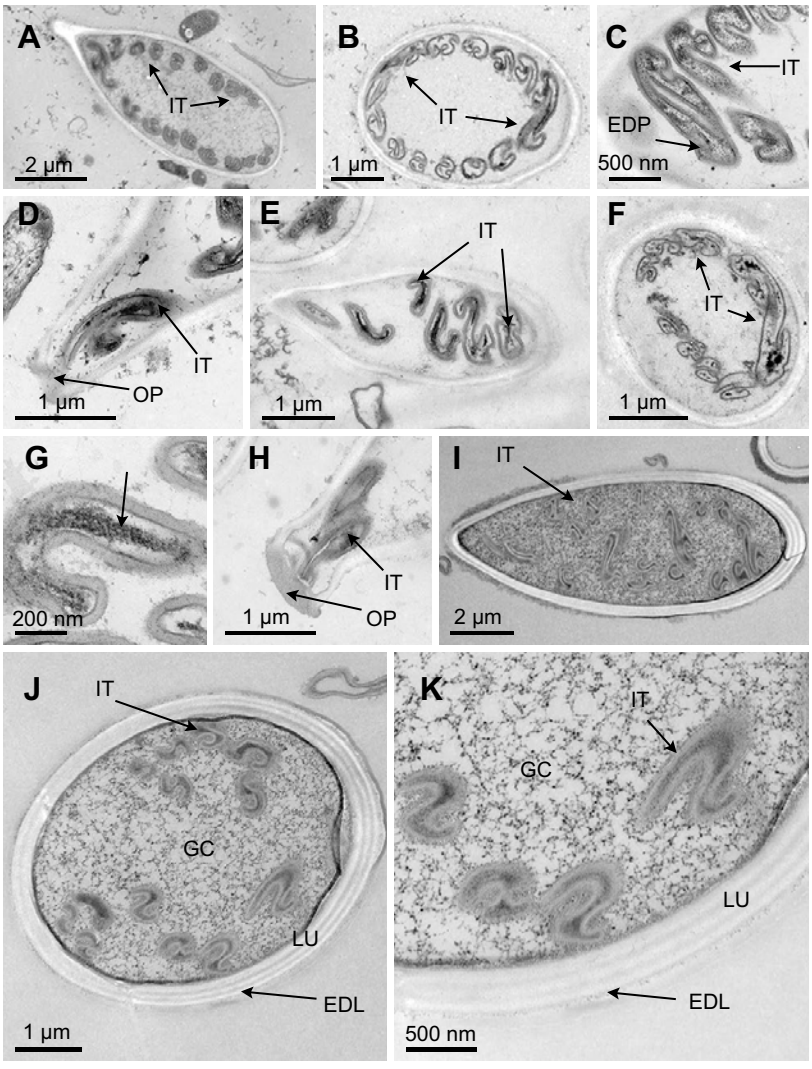

Fig. 3. Transmission electron micrographs of isolated nematocysts of the three parasites. (A–D) *Myxobolus honghuensis*. Longitudinal (A) and transverse (B) section of *M. honghuensis* nematocyst. (C) Electron-dense particles were observed in the tubule. (D) Opercular cap of *M. honghuensis* nematocyst. (E–H) *Myxobolus wulii*. Longitudinal (E) and transverse (F) section of *M. wulii* nematocyst. (G) At a higher magnification, it can been seen that the inverted tubule is hollow and filled with electron-dense particles. (H) Opercular cap of *M. wulii* nematocyst. (I–K) *Thelohanellus kitauei*. Longitudinal (I) and transverse (J) section of *T. kitauei*. (K) At a higher magnification, the nematocyst shows a trilaminar structure, with an outer electron-dense zone, an adjacent electron-lucent zone and an inner granular cortex. The electron-lucent zone can be further subdivided into at least three layers. ED, outer electron-dense zone; EDL, electron-dense layer; EDP, electron-dense particles; GC, inner granular cortex; IT, inverted tubule; LU, adjacent electron-lucent zone; OP, opercular cap.

zone and an inner granular cortex. The electron-lucent zone was further subdivided into at least three layers (Fig. 3J,K), which is consistent with former reports of an undissociated nematocyst ultrastructure (Guo et al., 2018). Collectively, these results suggest that isolated nematocysts are both structurally and functionally intact, which may benefit our understanding of them.

For shell valve isolation, a final 100% Percoll centrifugation at 6580 ***g*** for 15 min resulted in the optimal isolation of shell valves, to >98% purity in the upper part of the 100% layer (Fig. 1D). Repeating the process led to intact and clean shell valves (Fig. 2J–L). Likewise, in the case of nematocysts, the first attempt to isolate shell valves using 60%, 55%, 50%, 45%, 40% sucrose density gradient only produced shell valves with a maximum purity of 70% (Fig. S3A) and the density of the shell valves was speculated to be around 1.25753–1.28646 g ml^{-1}. The improved sucrose density gradient also produced non-optimal results of 80% purity (Fig. S3B). By resorting to the 80%, 100% Percoll gradient, the maximum purity of isolated shell valves was improved to 90% (Fig. S3C). These results also demonstrate the effectiveness of our protocol for shell valve isolation, which may facilitate resistance and immuno-protection studies of myxozoans.

In conclusion, our study presents a procedure for myxozoan dissection and validates it on three myxozoans. This method allows the isolation of nematocysts and shell valves at high yield and enables these extracts to be obtained free of host tissue. In addition, our protocol offers advantages in terms of cost, speed and effectiveness. Indeed, isolation of nematocysts and shell valves can be performed simultaneously and requires less than 2 h. As the separation of myxospore subunits is based solely on differences in density, with fine trial and error adjustment of the parameters, we see a high potential to extend this method to other myxozoans, or even other parasites. In subsequent studies, we will take advantage of the subunits obtained from the present protocol to acquire a deeper understanding of the cell biology and evolutionary significance of myxozoans.

Competing interests

The authors declare no competing or financial interests.

Author contributions

Conceptualization: Q.G., Y.L., Z.G.; Methodology: Y.L., Y.Z.; Investigation: Q.G., Y.L.; Resources: Q.G., Y.Z., Z.G.; Writing - original draft: Q.G., Z.G.; Writing - review & editing: Q.G., Y.L., Y.Z., Z.G.; Visualization: Q.G., Y.L., Z.G.; Supervision: Z.G.; Funding acquisition: Z.G.

Funding

This work was supported by Nature Science Foundation of China (grant nos. 31572233 and 31502209), China Agriculture Research System (grant no. CARS-46), the Hubei Agricultural Science and Technology Innovation Center (grant no. 2019-620-000-001-33) and Featuring Talents Cultivation Project (grant no. 4611300108).

Supplementary information

Supplementary information available online at
http://jeb.biologists.org/lookup/doi/10.1242/jeb.214916.supplemental

References

Aldama-Cano, D. J., Sanguanrut, P., Munkongwongsiri, N., Ibarra-Gámez, J. C., Itsathitphaisarn, O., Vanichviriyakit, R., Flegel, T. W., Sritunyalucksana, K. and Thitamadee, S. (2018). Bioassay for spore polar tube extrusion of shrimp *Enterocytozoon hepatopenaei* (EHP). *Aquaculture* **490**, 156-161. doi:10.1016/j.aquaculture.2018.02.039

Amberg, D. C., Burke, D. J. and Strathern, J. N. (2005). *Methods in Yeast Genetics: A Cold Spring Harbor Laboratory Course Manual*, 2005 edn. New York: Cold Spring Harbor Laboratory Press.

Atkinson, S. D., Bartholomew, J. L. and Lotan, T. (2018). Myxozoans: ancient metazoan parasites find a home in phylum Cnidaria. *Zoology* **129**, 66-68. doi:10.1016/j.zool.2018.06.005

Balasubramanian, P. G., Beckmann, A., Warnken, U., Schnölzer, M., Schüler, A., Bornberg-Bauer, E., Holstein, T. W. and Özbek, S. (2012). Proteome of *Hydra* nematocyst. *J. Biol. Chem.* **287**, 9672-9681. doi:10.1074/jbc.M111.328203

Ben-David, J., Atkinson, S. D., Pollak, Y., Yossifon, G., Shavit, U., Bartholomew, J. L. and Lotan, T. (2016). Myxozoan polar tubules display structural and functional variation. *Parasit. Vectors* **9**, 549. doi:10.1186/s13071-016-1819-4

Birsa, L. M., Verity, P. G. and Lee, R. F. (2010). Evaluation of the effects of various chemicals on discharge of and pain caused by jellyfish nematocysts. *Comp. Biochem. Physiol. C Toxicol. Pharmacol.* **151**, 426-430. doi:10.1016/j.cbpc.2010.01.007

Brinkman, D. L., Jia, X., Potriquet, J., Kumar, D., Dash, D., Kvaskoff, D. and Mulvenna, J. (2015). Transcriptome and venom proteome of the box jellyfish *Chironex fleckeri*. *BMC Genomics* **16**, 407. doi:10.1186/s12864-015-1568-3

Coppens, I. (2019). Robbing host phosphatidic acid to survive: a strategy of a fly parasite. *Trends Parasitol.* **35**, 336-338. doi:10.1016/j.pt.2019.03.006

Dunkley, P. R., Jarvie, P. E., Heath, J. W., Kidd, G. J. and Rostas, J. A. P. (1986). A rapid method for isolation of synaptosomes on Percoll gradients. *Brain Res.* **372**, 115-129. doi:10.1016/0006-8993(86)91464-2

Dyková, I., Tyml, T. and Kostka, M. (2011). Xenoma-like formations induced by *Soricimyxum fegati* (Myxosporea) in three species of shrews (Soricomorpha: Soricidae), including records of new hosts. *Folia Parasitol.* **58**, 249-256. doi:10.14411/fp.2011.024

Glaser, O. C. and Sparrow, C. M. (1909). The physiology of nematocysts. *J. Exp. Zool.* **6**, 361-382. doi:10.1002/jez.1400060303

Goodgame, R. W. (1996). Understanding intestinal spore-forming protozoa: cryptosporidia, microsporidia, cyclospora. *Ann. Intern. Med.* **124**, 429-441. doi:10.7326/0003-4819-124-4-199602150-00008

Guo, Q., Huang, M., Liu, Y., Zhang, X. and Gu, Z. (2018). Morphological plasticity in *Myxobolus* Bütschli, 1882: a taxonomic dilemma case and renaming of a parasite species of the common carp. *Parasit. Vectors* **11**, 399. doi:10.1186/s13071-018-2943-0

Halldorsson, S., Lucumi, E., Gómez-Sjöberg, R. and Fleming, R. M. T. (2015). Advantages and challenges of microfluidic cell culture in polydimethylsiloxane devices. *Biosens. Bioelectron.* **63**, 218-231. doi:10.1016/j.bios.2014.07.029

Hoffman, G. L., Putz, R. E. and Dunbar, C. E. (1965). Studies on *Myxosoma cartilaginis* n. sp. (Protozoa: Myxosporidea) of centrarchid fish and a synopsis of the *Myxosoma* of North American freshwater fishes. *J. Protozool.* **12**, 319-332. doi:10.1111/j.1550-7408.1965.tb03220.x

Honig, P. (2013). *Principles of Sugar Technology*. Amsterdam: Elsevier.

Jaroenlak, P., Boakye, D. W., Vanichviriyakit, R., Williams, B. A. P., Sritunyalucksana, K. and Itsathitphaisarn, O. (2018). Identification, characterization and heparin binding capacity of a spore-wall, virulence protein from the shrimp microsporidian, *Enterocytozoon hepatopenaei* (EHP). *Parasit. Vectors* **11**, 177. doi:10.1186/s13071-018-2758-z

Marino, A., Di Paola, R., Crisafulli, C., Mazzon, E., Morabito, R., Paterniti, I., Galuppo, M., Genovese, T., La Spada, G. and Cuzzocrea, S. (2009). Protective effect of melatonin against the inflammatory response elicited by crude venom from isolated nematocysts of *Pelagia noctiluca* (Cnidaria, Scyphozoa). *J. Pineal Res.* **47**, 56-69. doi:10.1111/j.1600-079X.2009.00688.x

Mark, D., Haeberle, S., Roth, G., Von Stetten, F. and Zengerle, R. (2010). Microfluidic lab-on-a-chip platforms: requirements, characteristics and applications. In *Microfluidics Based Microsystems*. NATO Science for Peace and Security Series A: Chemistry and Biology (ed. S. Kakaç, B. Kosoy, D. Li and A. Pramuanjaroenkij), pp. 305-376. Springer.

Molnár, K., Székely, C., Hallett, S. L. and Atkinson, S. D. (2009). Some remarks on the occurrence, host-specificity and validity of *Myxobolus rotundus* Nemeczek, 1911 (Myxozoa: Myxosporea). *Syst. Parasitol.* **72**, 71-79. doi:10.1007/s11230-008-9161-7

Morabito, R., Marino, A. and La Spada, G. (2013a). Heavy metals affect regulatory volume decrease (RVD) in nematocysts isolated from the jellyfish *Pelagia noctiluca*. *Comp. Biochem. Physiol. A. Mol. Integr. Physiol.* **165**, 199-206. doi:10.1016/j.cbpa.2013.03.004

Morabito, R., Marino, A., Lauf, P. K., Adragna, N. C. and La Spada, G. (2013b). Sea water acidification affects osmotic swelling, regulatory volume decrease and discharge in nematocytes of the jellyfish *Pelagia noctiluca*. *Cell. Physiol. Biochem.* **32**, 77-85. doi:10.1159/000356629

Morabito, R., Marino, A., Dossena, S. and La Spada, G. (2014). Nematocyst discharge in *Pelagia noctiluca* (Cnidaria, Scyphozoa) oral arms can be affected by lidocaine, ethanol, ammonia and acetic acid. *Toxicon* **83**, 52-58. doi:10.1016/j.toxicon.2014.03.002

Morsy, K., Semmler, M., Al-Olayan, E. and Mehlhorn, H. (2016). *Henneguya collaris* sp. nov., (Myxosporidia), parasite of the Greenband Parrotfish *Scarus collana* Rüppell, 1835 (Actinopterygii, Scaridae) from the Red Sea, Egypt. A light and electron microscopic study. *Parasitol. Res.* **115**, 2253-2261. doi:10.1007/s00436-016-4968-7

Naldoni, J., Adriano, E. A., Hartigan, A., Sayer, C. and Okamura, B. (2019). Malacosporean myxozoans exploit a diversity of fish hosts. *Parasitology* **146**, 968-978. doi:10.1017/S0031182019000246

Okamura, B., Gruhl, A. and Bartholomew, J. L. (2015). *Myxozoan Evolution, Ecology and Development*. Cham: Springer International Publishing.

Piriatinskiy, G., Atkinson, S. D., Park, S., Morgenstern, D., Brekhman, V., Yossifon, G., Bartholomew, J. L. and Lotan, T. (2017). Functional and proteomic analysis of *Ceratonova shasta* (Cnidaria: Myxozoa) polar capsules reveals adaptations to parasitism. *Sci. Rep.* **7**, 9010. doi:10.1038/s41598-017-09955-y

Ponce, D., Brinkman, D., Potriquet, J. and Mulvenna, J. (2016). Tentacle transcriptome and venom proteome of the pacific sea nettle, *Chrysaora fuscescens* (Cnidaria: Scyphozoa). *Toxins* **8**, 102. doi:10.3390/toxins8040102

Schlesinger, A., Zlotkin, E., Kramarsky-Winter, E. and Loya, Y. (2008). Cnidarian internal stinging mechanism. *Proc. R. Soc. B Biol. Sci.* **276**, 1063-1067. doi:10.1098/rspb.2008.1586

Vávra, J., Hyliš, M., Fiala, I. and Nebesářová, J. (2016). *Globulispora mitoportans* n. g., n. sp., (Opisthosporidia: Microsporidia) a microsporidian parasite of daphnids with unusual spore organization and prominent mitosome-like vesicles. *J. Invertebr. Pathol.* **135**, 43-52. doi:10.1016/j.jip.2016.02.003

Velve-Casquillas, G., Le Berre, M., Piel, M. and Tran, P. T. (2010). Microfluidic tools for cell biological research. *Nano Today* **5**, 28-47. doi:10.1016/j.nantod.2009.12.001

Xu, Y., Takvorian, P., Cali, A., Wang, F., Zhang, H., Orr, G. and Weiss, L. M. (2006). Identification of a new spore wall protein from *Encephalitozoon cuniculi*. *Infect. Immun.* **74**, 239-247. doi:10.1128/IAI.74.1.239-247.2006

Yang, D., Pan, L., Peng, P., Dang, X., Li, C., Li, T., Long, M., Chen, J., Wu, Y. and Du, H. (2017). Interaction between SWP9 and polar tube proteins of the microsporidian *Nosema bombycis* and function of SWP9 as a scaffolding protein contribute to polar tube tethering to the spore wall. *Infect. Immun.* **85**, e00872-16. doi:10.1128/IAI.00872-16

Yang, D., Pan, L., Chen, Z., Du, H., Luo, B., Luo, J. and Pan, G. (2018). The roles of microsporidia spore wall proteins in the spore wall formation and polar tube anchorage to spore wall during development and infection processes. *Exp. Parasitol.* **187**, 93-100. doi:10.1016/j.exppara.2018.03.007